Development 134, 1045-1050 (2007) doi:10.1242/dev.02774

Plants expressing a *miR164*-resistant *CUC2* gene reveal the importance of post-meristematic maintenance of phyllotaxy in *Arabidopsis*

Alexis Peaucelle, Halima Morin, Jan Traas and Patrick Laufs*

In plants, the arrangement of organs along the stem (phyllotaxy) follows a predictable pattern. Recent studies have shown that primordium position at the meristem is governed by local auxin gradients, but little is known about the subsequent events leading to the phyllotaxy along the mature stem. We show here that plants expressing a *miR164*-resistant *CUP-SHAPED COTYLEDON2* (*CUC2*) gene have an abnormal phyllotactic pattern in the fully grown stem, despite the pattern of organ initiation by the meristem being normal. This implies that abnormal phyllotaxy is generated during stem growth. These plants ectopically express *CUC2* in the stem, suggesting that the proper timing of *CUC2* expression is required to maintain the pattern initiated in the meristem. Furthermore, by carefully comparing the phyllotaxy in the meristem and along the mature inflorescence in wild types, we show that such deviation also occurs during wild-type development, although to a smaller extent. We therefore suggest that the phyllotactic pattern in a fully grown stem results not only from the organogenetic activity of the meristem, but also from the subsequent growth pattern during stem development.

KEY WORDS: Phyllotaxy, CUP-SHAPED COTYLEDON, Boundary domain, Internode, miRNA, *Arabidopsis*

INTRODUCTION

A feature of plant architecture that has puzzled scientists for centuries is the strikingly regular position of the lateral organs along the stem. A group of undifferentiated cells – the shoot apical meristem (SAM) – plays a crucial role in the formation of this pattern by initiating organ primordia on its flanks in a temporally and spatially controlled manner. The mechanisms controlling organ positioning in the SAM (hereafter referred to as the meristematic phyllotaxy) are beginning to be unravelled (Reinhardt, 2005). Little is known, however, about the maintenance of relative organ position during the subsequent growth and differentiation of the shoot and the generation of the final phyllotaxy (hereafter referred to as the phyllotactic pattern) (Reinhardt, 2005).

Many mutants with abnormal phyllotactic patterns have been described. The *bellringer* [*blr*; also known as *larson* (*lsn*), *pennywise* (*pny*) and *vaamana* (*van*)] mutant (Bhatt et al., 2004; Byrne et al., 2003; Smith and Hake, 2003) has internodes of variable lengths, some being very short and resulting in the formation of organ clusters. The positions of the organs in the meristems of *blr* mutants are abnormal, although the meristem appears to have a normal shape and size (Byrne et al., 2003). This contrasts with most mutants, in which abnormal meristem size or organisation lead to defects in organ position from their initiation onwards (Chaudhury et al., 1993; Clark et al., 1993; Clark et al., 1995; Jeong et al., 1999; Moussian et al., 1998; Para and Sundas-Larsson, 2003).

Here, we describe a novel mechanism leading to changes in phyllotactic pattern. The *CUC2* gene, together with two other members of the NAC family of transcription factors – *CUC1* and *CUC3* – are required for the specification of the boundary domain surrounding organ primordia (Aida et al., 1997; Takada et al., 2001; Vroemen et al., 2003). *miR164* is a microRNA (miRNA) that targets the transcript of the *CUC1* and *CUC2* genes for endonucleotide cleavage, a role that is important during the development of the organ boundaries, flowers and leaves (Baker et al., 2005; Kasschau et al., 2003; Laufs et al., 2004; Mallory et al., 2004; Nikovics et al., 2006; Rhoades et al., 2002). We show here that plants expressing a *miR164*-resistant *CUC2* gene show abnormal phyllotactic patterns due to post-meristematic perturbations of stem growth. Furthermore, in wild-type plants, the position of the organs along the mature stem is more variable than in the meristem, suggesting that variability in the phyllotaxy also occurs during wild-type stem development, although to a smaller degree. This shows that the phyllotaxy initiated at the meristem has to be maintained during stem growth and differentiation, and suggests that this requires the proper timing of *CUC2* expression.

MATERIALS AND METHODS

Plant material and growth conditions

CUC2g-m4 and *CUC2-wt* transgenic plants (Nikovics et al., 2006), and the *LFY::ALCR alcA::erGFP* (Deveaux et al., 2003) and *DR5::GFP* (Benkova et al., 2003) lines have all been described previously. Plant growth in controlled chambers was conducted according to Laufs et al. (Laufs et al., 2003) and ethanol induction according to Deveaux et al. (Deveaux et al., 2003).

Phyllotactic pattern and meristematic phyllotaxy measurements

Phyllotactic pattern was assessed on fully grown stems of 2-month-old plants. The top 5 cm of the stem was not assessed, as elongation was incomplete. Divergence angle and internode length were measured simultaneously, using the device presented in Fig. S1A in the supplementary material. The divergence angle was measured between the insertion points of two successive floral pedicels and is therefore independent of the outgrowth direction of the pedicel (see Fig. S1B in the supplementary material). Phyllotaxy orientation can be either clockwise or anticlockwise. For each individual, the phyllotaxy orientation was set to the direction giving the smallest average divergence angle.

Laboratoire de Biologie Cellulaire UR501, Institut J. P. Bourgin, INRA, F-78000 Versailles, France.

*Author for correspondence (e-mail: laufs@versailles.inra.fr)

Accepted 5 December 2006

To analyse the meristematic phyllotaxy, we determined the order of primordium formation by studying phyllotaxy in plants producing erGFP under the control of the primordium marker LFY. GFP observations were made with a Leica MZFIII fluorescence stereomicroscope with a 450-490 nm excitation filter set and a 525-550 nm bandpass, or with a 480 nm long-pass emission filter set. Digital pictures were taken with a Nikon Coolpix995 camera. The divergence angle at the meristem was measured using Optimas software (version: 6.51.199, Media Cybernetics).

The distributions were compared using the Kolmogorov-Smirnov test (K-S test) at http://home.ubalt.edu/ntsbarsh/Business-stat/otherapplets/ks.htm.

Epidermal cell- and meristem-structure observations

Epidermal cells were observed on an imprint produced by applying transparent nail polish to the surface of the plant. Digital pictures were taken with a Nikon Coolpix995 camera. Cell length was measured with Optimas software (version: 6.51.199, Media Cybernetics). Cell length that was measured at the two ends and in the middle of the internode was found to be uniform. Therefore, the number of cells per internode in a row of cells could be calculated by dividing the internode length by the cell length.

Meristem size and structure were analysed on partially dissected and cleared apices. Alternatively, sections of paraffin-embedded material were observed.

Scanning electron microscopy

Scanning electron microscopy was carried out as previously described (Bertrand et al., 2003).

In situ hybridisation

CUC2 in situ hybridisation was performed as described by Nikovics et al. (Nikovics et al., 2006).

RESULTS AND DISCUSSION

Plants expressing a *miR164*-resistant *CUC2* gene have an abnormal phyllotactic pattern

Plants expressing a *miR164*-resistant *CUC2* gene (*CUC2g-m4*) showed multiple phenotypical defects, including serrated leaves, enlarged boundaries around the floral organs and defects in carpel development (Nikovics et al., 2006). In addition, they showed abnormal phyllotaxy defects (Fig. 1). Out of the 60 *CUC2g-m4* lines that we generated (11 and 49 in the Col and WS backgrounds, respectively), three showed extremely compact inflorescences with very short internodes and long floral pedicels (Fig. 1C). None of the 52 *CUC2g-wt* control lines (21 and 31 in the Col and WS backgrounds, respectively) that were transformed with an unmodified *CUC2* gene had such a phenotype. Weaker *CUC2g-m4* lines also showed abnormal inflorescence architecture. In wild-type *Arabidopsis*, a cauline leaf subtends the side branches. By contrast, one or two additional smaller leaves growing on the sides of the normal cauline leaves were frequently observed in *CUC2g-m4* lines (32%) and less often in *CUC2g-wt* lines (12%) (Fig. 1A,B). In the *Arabidopsis* inflorescence, organs are arranged following a spiral pattern. Organs of *CUC2g-m4* lines showed a less regular distribution along the inflorescence (Fig. 1D,E). In some cases, flowers formed clusters that were separated with longer internodes (Fig. 1D,E). There was no strict separation between these two types of abnormal phyllotactic pattern, as siblings of the same transgenic lines could show either phenotype and individual plants could show both phenotypes at different moments of their development. This suggests that these variations are extremely sensitive to the level of *CUC2* expression. These modifications were observed in at least 17 independent *CUC2g-m4* transgenic lines (two and 15 in the Col and WS backgrounds, respectively), but in none of the *CUC2g-wt* lines.

Precise characterisation of the phyllotactic pattern in wild-type and *CUC2g-m4* plants

We characterised the phyllotactic pattern of the flowers by measuring the divergence angle and internode length between successive organs along the main inflorescence stem (Fig. 1F, and see Fig. S2 in the supplementary material). The divergence angle was measured between the insertion points of the pedicel of two successive organs and is therefore independent from the growth direction of the flower (see Fig. S1 in the supplementary material for details). For each inflorescence, we determined the orientation of the generative spiral and measured divergence angles according to this orientation.

In wild-type WS, the mean divergence angle (149°, n=217) was surprisingly far from the theoretical angle of 137.5°, and we also observed considerable variability (Fig. 1F). Only 48% of the divergence angles fell into the 120-150° class, which contains the theoretical angle. This proportion increased to 82% if the class was enlarged to encompass angles ranging from 90-180°. In total, 18% of the measured angles fell outside of this class, with a second maximum in the angle distribution observed for the 210-300° class, which contained 11.5% of all of the measured angles. The expected angle in the case of the reversal of the direction of phyllotaxy (360°-137.5°=222.5°) falls into this class, suggesting that the phyllotactic pattern may have been transiently reversed. Most of the divergence angles falling into this 210-300° class were not isolated. Instead, they formed groups of three to 11 successive angles in 65% of cases. This observation is consistent with the transient inversion of phyllotaxy orientation, followed by a reversion to the original orientation.

Internode length was highly variable in WS, ranging from less than 0.5 mm to 2 cm, and no major class of internode length could be identified (Fig. 1F). No correlation was observed between internode length and divergence angle (see Fig. S3 in the supplementary material). Thus, abnormal divergence angles are not preferentially associated with a decrease or an increase in internode length.

From this, we concluded that the phyllotactic pattern is to some extent variable in wild-type WS *Arabidopsis*. We observed a similar variability in the phyllotactic pattern of plants grown under three other environmental conditions, including growth chambers (see Fig. S4 in the supplementary material). This suggests that the variability is unlikely to result from some particularity or from variations in the environment. In addition, variability of the phyllotactic pattern was also observed in a second ecotype, Col (see Fig. S2 in the supplementary material). Altogether, this suggests that the observed variability is an intrinsic property of the phyllotactic pattern of *Arabidopsis*.

We next examined two representative *CUC2g-m4* transgenic lines (Fig. 1F, and see Fig. S2 in the supplementary material). The WS *CUC2g-m4* line had a strong increase in the frequency of short internodes (77% less than 3 mm, versus 19% in wild type), which accounts for the organ clusters. Long internodes were also more frequent (6% greater than 2.1 cm, versus 1.5% in wild type). The divergence-angle distribution was also strongly affected, as the maximum in the 90-180° class observed in wild type was not observed in the mutant, which showed a more uniform distribution (Fig. 1F). Similar changes of the internode length and divergence angle were observed in the Col *CUC2g-m4* line (see Fig. S2 in the supplementary material).

Meristem function is unaffected in *CUC2g-m4* plants

Because abnormal phyllotactic pattern is often associated with perturbed meristem size or organisation, we analysed the meristem of *CUC2g-m4* plants. Meristems of transgenic plants showed typical layered organisation (Fig. 2A) and their size was not modified compared to the wild-type control (Fig. 2B).

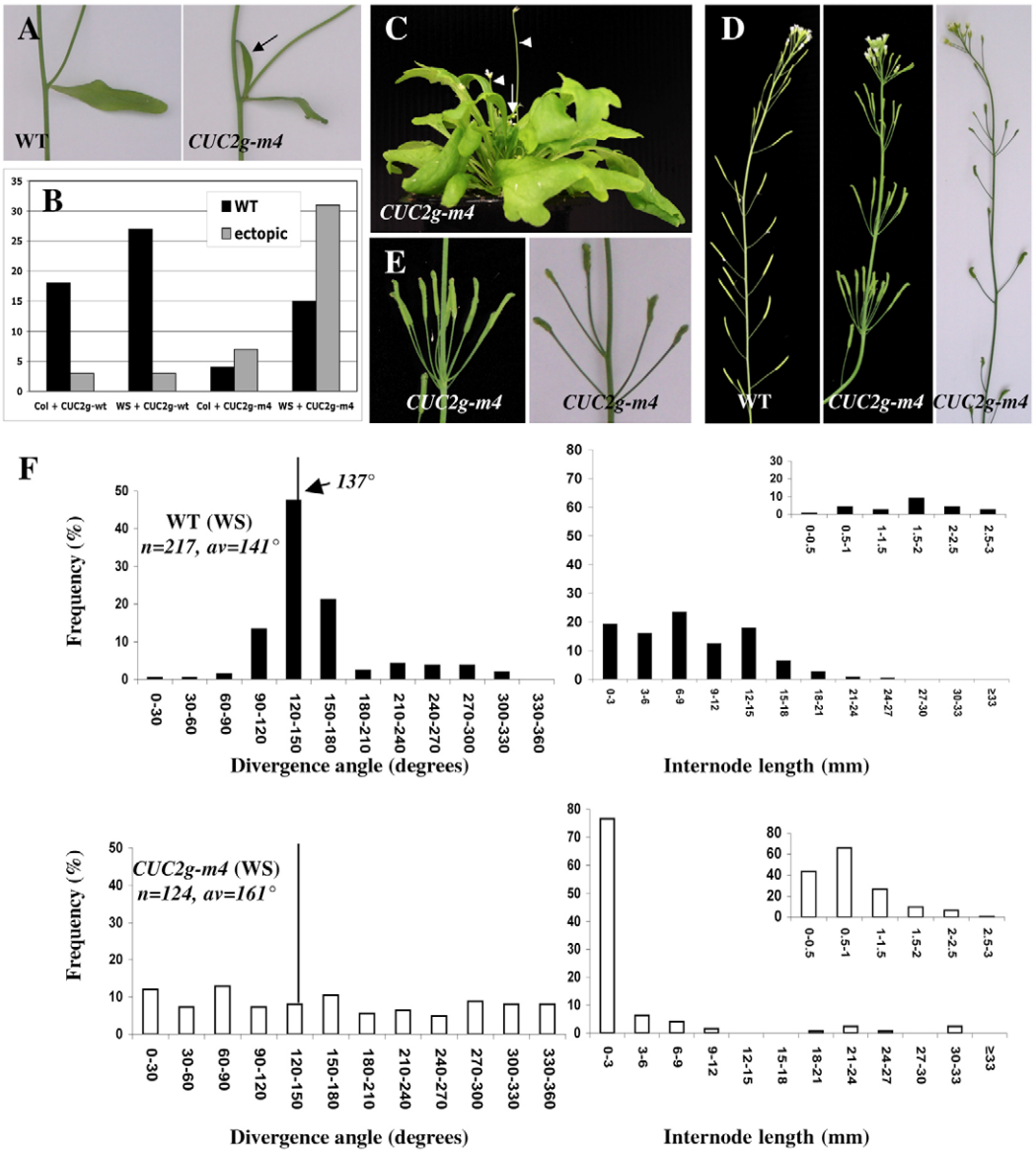

Fig. 1. Phyllotactic pattern in *CUC2g-m4* and wild type. (**A**) Axillary region. An additional leaf develops in the axils of *CUC2g-m4* plants (arrow). (**B**) Frequency of the extra leaf phenotype in independent transgenic lines. (**C**) Strong *CUC2g-m4* plants with an extreme reduction of the inflorescence (arrow) and of flowers with long pedicels (arrowhead). (**D**) Inflorescence of wild-type and representative *CUC2g-m4* plants showing an abnormal phyllotactic pattern. (**E**) Close-up of D. (**F**) Detailed analysis of the phyllotactic pattern in wild-type and *CUC2g-m4* plants (WS background, see Fig. S2 in the supplementary material for Col). Left: distribution of divergence angle between two successive flowers along the stem. Percentages of total divergence angles measured (*n*) that fell into 12 classes, each of 30°, and the averages (*av*) are shown. Right: distribution of internode length between two successive flowers along the stem. Percentages of total internode lengths that fell into classes of 3 mm each are shown. Insets show a finer distribution of internodes that were less than 3 mm long, in classes of 0.5 mm. Notice that the scale is different for the insets.

Variability in divergence angle principally results from post-meristematic defects

Because the meristem appeared to be unaffected in the *CUC2g-m4* lines, we next analysed primordium initiation. As auxin has been implicated in the control of the primordium initiation site in the meristem (de Reuille et al., 2006; Jonsson et al., 2006; Reinhardt et al., 2000; Reinhardt et al., 2003; Smith et al., 2006; Vernoux et al., 2000), we first analysed auxin response using an auxin-sensitive promoter (DR5) controlling the expression of a GFP reporter gene (Benkova et al., 2003). In both wild-type and *CUC2g-m4* meristems, similar strong GFP staining was observed in two to three distinct groups of cells (Fig. 2C). This suggests that the auxin-response peaks associated with primordium initiation are not disturbed in *CUC2g-m4* apices.

We next analysed meristematic phyllotaxy, using GFP expression under the control of the *LFY* promoter to stage the primordia. The divergence-angle distribution in the meristem of *CUC2g-m4* plants was not significantly different from that observed in the wild type (K-S test, $P=0.04$), indicating that meristematic phyllotaxy was normal in *CUC2g-m4* apices (Fig. 2D). Comparison of the *CUC2g-m4* meristematic phyllotaxy (Fig. 2D) with the phyllotactic pattern (Fig. 1F) indicates that most of the variability of the phyllotactic

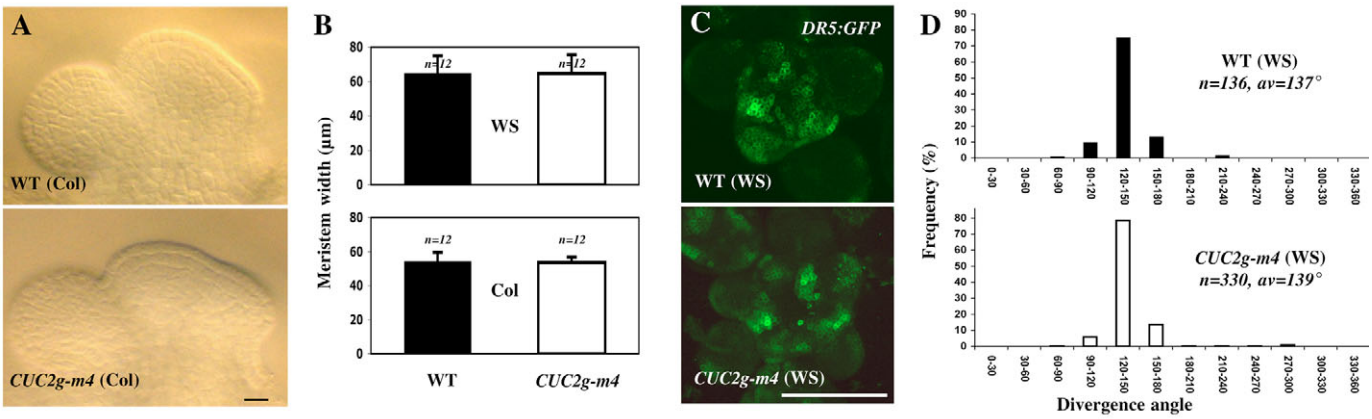

Fig. 2. Meristems and meristematic phyllotaxy are unaltered in *CUC2g-m4* plants. (**A**) Cleared inflorescence meristems of wild type and *CUC2g-m4* (Col background). (**B**) Meristem width of wild type and *CUC2g-m4* in WS and Col backgrounds. Number of individuals measured (*n*) and standard deviations (bars) are indicated. (**C**) Expression of the auxin response sensor *DR5:GFP in* wild type and *CUC2g-m4* (WS background). (**D**) Meristematic phyllotaxy in wild type and *CUC2g-m4* (WS background; see Fig. S2 in the supplementary material for Col). Percentages of total measurements (n) of divergence angle between two successive flowers in the meristem falling into twelve 30° classes and averages (*av*) are shown. Scale bars: 10 μm in A; 100 μm in C.

patterns occurs after the initiation of the primordia at the meristem. Similar conclusions could be drawn from the analysis of the Col *CUC2g-m4* line (see Fig. S2 in the supplementary material). Interestingly, the distribution of divergence angles in the apex of wild-type plants was significantly different (K-S test, P=0.21) and was sharper than the distribution of divergence angles on the stem. This indicates that, as in *CUC2g-m4* plants, variability of the phyllotactic pattern is generated during wild-type stem growth, although to a lesser extent than in the transgenic lines.

Clusters of flowers in *CUC2g-m4* plants do not result from the simultaneous initiation of flower primordia

We then determined whether the observed organs clusters resulted from the simultaneous initiation of several flower primordia or from the inhibition of internode growth. We reasoned that, if the flowers from a cluster were initiated together, they should be at similar developmental stages. This was not the case (Fig. 3A). We also directly analysed the initiation of primordia on apices expressing the GFP reporter under the control of the *LFY* promoter. In wild-type and *CUC2g-m4* plants, the flower primordia were all at different developmental stages, reflecting their regular timing of initiation. Altogether, these observations showed that the clusters do not result from simultaneous initiation of several organs but from reduced internode growth.

In order to identify the point at which internode development in *CUC2g-m4* plants deviated from that in wild type, we observed internodes on partially dissected inflorescences (Fig. 3B). Internode length increased gradually and regularly down the stem in wild-type plants, whereas it was more variable in *CUC2g-m4* inflorescences. Interestingly, this variability between internodes on the same stem became clear in the subapical region. This suggested that abnormal internode length mainly resulted from post-meristematic defects in internode growth.

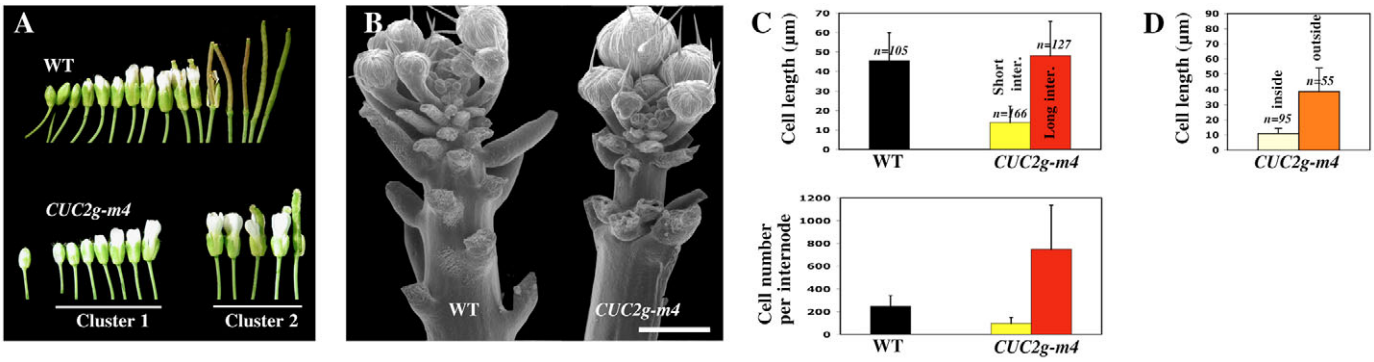

Fig. 3. Short internodes in *CUC2g-m4* result from a post-meristematic reduction of growth due to a combination of fewer and smaller cells. (**A**) Developmental series of flowers along the stem. Flowers are ordered from the top (left) to the bottom (right) of the inflorescence stem. Not all of the flowers of a *CUC2g-m4* cluster (underlined) are at the same stage. (**B**) SEM views of the early phases of inflorescence development. Inflorescences were partially dissected to reveal the internodes. (**C**) Epidermal cell length and number of wild-type (10 mm long), short *CUC2g-m4* (less than 1 mm long, yellow bars) or long *CUC2g-m4* (30 mm long, red bars) internodes. Cell numbers per internode were calculated based on cell and internode lengths. Number of individuals measured (*n*) and standard deviations (bars) are indicated. (**D**) Epidermal cell size was measured on either the inside or the outside of twisted *CUC2g-m4* stems. Scale bar: 0.5 mm in B.

Variability of internode length in *CUC2g-m4* plants is due to changes in both cell number and cell size

We investigated the cellular basis of variation in internode length by measuring epidermal-cell length and calculating the cell number on wild-type internodes (mean size 10 mm), and on long (mean size 30 mm) and short (less than 1 mm) internodes of *CUC2g-m4* plants (Fig. 3C). The long *CUC2g-m4* internodes were formed by approximately 3-times more cells, which all had normal lengths (Fig. 3C). The short internode of *CUC2g-m4* plants contained approximately 2.5 fewer cells, which were only about a third the wild-type length. If cell elongation and division are variable in the inflorescence, it would be expected that an asymmetrical distribution of regions of shorter cells or longer cells leads to the twisting of the inflorescence. Such twisting was observed in *CUC2g-m4* plants and the cells on the inner part were shorter than those on the outer part of the twisted stem (Fig. 3D). We therefore conclude that internode-length variation results from a combination of cell-elongation and cell-division defects.

Abnormal internode length in *CUC2g-m4* plants is associated with ectopic *CUC2* expression during stem growth

In wild-type plants, *CUC2* was expressed in a narrow group of cells that formed the boundary domain between the young flower primordia and the inflorescence meristem (Fig. 4A). Once the flower started to grow out and the internode began to elongate, *CUC2* expression was restricted to the axils of the floral pedicels and was maintained there for several nodes. No *CUC2* expression could be detected in the internode.

C*UC2g-m4* plants showed an increase in the level of *CUC2* expression, as well as a severely modified expression pattern (Fig. 4B). The number of cells expressing *CUC2* in the meristem was increased, which is consistent with an enlargement of the boundary domain. *CUC2* expression was maintained for longer in the axils of the floral pedicels during stem development compared to wild type, as it was detected in lower nodes. *CUC2* expression also expanded in the adaxial region of the flower pedicel. *CUC2* was expressed in the epidermal and cortical cells of the internode. Twisted *CUC2g-m4* stems showed an asymmetrical distribution of *CUC2* expression, with maximum expression on the inner part of the bent stem (Fig. 4C,D).

These observations show that, in the apex, all cells between two flowers initially express *CUC2*. These *CUC2*-expressing cells are the source for the internode and node cells. During later stages, a region with no *CUC2* expression appears and grows rapidly (the internode), while *CUC2* expression is maintained for slightly longer in the axils of the flower pedicels. Thus, differentiation of the internodes involves the establishment of a cell population that no longer expresses *CUC2*. *miR164* has a central role in the clearing of *CUC2* mRNA from internode cells, as *CUC2g-m4* plants show ectopic *CUC2* mRNA accumulation in the internode. We suggest that post-meristematic changes of the phyllotaxy result from this ectopic expression of *CUC2* in cells derived from the boundary domain and that give rise to the internode. How could this occur? It has been suggested that *CUC2* genes repress growth during embryogenesis, resulting in the formation of two separated cotyledons (Aida et al., 1997; Aida et al., 1999). The enhanced reduction of internode elongation in strong *CUC2g-m4* plants (Fig. 1C) and the reduction of stem growth on the side with the strongest *CUC2* expression (Fig. 4C,D) suggest a similar CUC2-mediated growth inhibition.

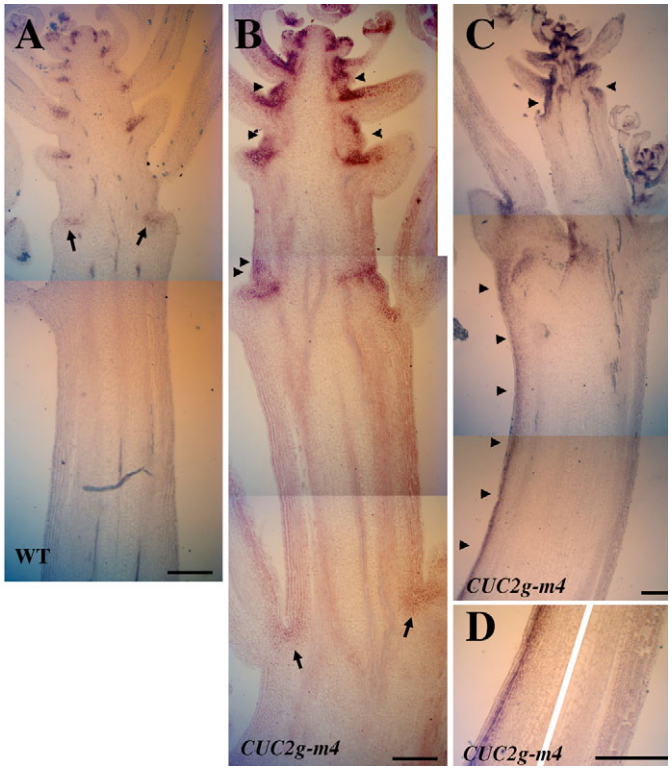

Fig. 4. *CUC2* in situ hybridisation on longitudinal sections of inflorescence apices. (**A**) Wild type. (**B**,**C**,**D**) *CUC2g-m4* transgenic plants. (C) Twisted stem with *CUC2* expression on the inner side. (D) Close-up of the inner and outer sides of C. Arrows point to the lowest axils with detectable *CUC2* expression. Arrowheads indicate ectopic *CUC2* in the internodes. Scale bars: 100 μm.

CONCLUSION

By characterising plants expressing a *CUC2* gene modified to be resistant to the microRNA *miR164*, we show that an abnormal phyllotactic pattern can be generated despite the plants having an initial normal meristematic phyllotaxy. Interestingly, wild-type *Arabidopsis* showed some variability in the phyllotactic pattern, whereas the meristematic phyllotaxy was more robust. This indicates that, in the transgenics, and to a lower level in the wild type, variability of the phyllotaxy is generated during stem growth. We therefore suggest that the phyllotactic pattern in the fully grown stem results not only from the organogenetic activity of the meristem, but also from subsequent events during stem growth. This pattern may either be well-maintained (as in wild-type *Arabidopsis*) or be maintained less efficiently (as in *CUC2g-m4* plants). Furthermore, our work shows that rapid clearing of the *CUC2* transcript from internode cells is required for the efficient maintenance of the phyllotactic pattern during stem development.

We thank D. Barabé and B. Jeune for discussion on the analysis of the phyllotaxy; R. Simon, M. Aida, V. Pautot, J. D. Faure and J. C. Palauqui for discussions; B. Letarnec for plant care; O. Grandjean for help with the confocal microscope; and S. Domenichini for SEM assistance. This work was partially supported by an ACI Jeunes Chercheurs award to P.L. and by the trilateral Genoplante GENOSOME program TRIL-046.

Supplementary material

Supplementary material for this article is available at http://dev.biologists.org/cgi/content/full/134/6/1045/DC1

References

Aida, M., Ishida, T., Fukaki, H., Fujisawa, H. and Tasaka, M. (1997). Genes involved in organ separation in Arabidopsis: an analysis of the cup-shaped cotyledon mutant. *Plant Cell* **9**, 841-857.

Aida, M., Ishida, T. and Tasaka, M. (1999). Shoot apical meristem and cotyledon formation during Arabidopsis embryogenesis: interaction among the CUP-SHAPED COTYLEDON and SHOOT MERISTEMLESS genes. *Development* **126**, 1563-1570.

Baker, C. C., Sieber, P., Wellmer, F. and Meyerowitz, E. M. (2005). The early extra petals1 mutant uncovers a role for microRNA miR164c in regulating petal number in Arabidopsis. *Curr. Biol.* **15**, 303-315.

Benkova, E., Michniewicz, M., Sauer, M., Teichmann, T., Seifertova, D., Jurgens, G. and Friml, J. (2003). Local, efflux-dependent auxin gradients as a common module for plant organ formation. *Cell* **115**, 591-602.

Bertrand, C., Bergounioux, C., Domenichini, S., Delarue, M. and Zhou, D. X. (2003). Arabidopsis histone acetyltransferase AtGCN5 regulates the floral meristem activity through the WUSCHEL/AGAMOUS pathway. *J. Biol. Chem.* **278**, 28246-28251.

Bhatt, A. M., Etchells, J. P., Canales, C., Lagodienko, A. and Dickinson, H. (2004). VAAMANA–a BEL1-like homeodomain protein, interacts with KNOX proteins BP and STM and regulates inflorescence stem growth in Arabidopsis. *Gene* **328**, 103-111.

Byrne, M. E., Groover, A. T., Fontana, J. R. and Martienssen, R. A. (2003). Phyllotactic pattern and stem cell fate are determined by the Arabidopsis homeobox gene BELLRINGER. *Development* **130**, 3941-3950.

Chaudhury, A. M., Letham, S., Craig, S. and Dennis, E. S. (1993). *amp1*: a mutant with high cytokinin levels and altered embryonic pattern, faster vegetative growth, constitutive photomorphogenesis and precocious flowering. *Plant J.* **4**, 907-916.

Clark, S. E., Running, M. P. and Meyerowitz, E. M. (1993). CLAVATA1, a regulator of meristem and flower development in Arabidopsis. *Development* **119**, 397-418.

Clark, S. E., Running, M. P. and Meyerowitz, E. M. (1995). *CLAVATA3* is a specific regulator of shoot meristem development affecting the same processes as *CLAVATA1*. *Development* **121**, 2057-2067.

de Reuille, P. B., Bohn-Courseau, I., Ljung, K., Morin, H., Carraro, N., Godin, C. and Traas, J. (2006). Computer simulations reveal properties of the cell-cell signaling network at the shoot apex in Arabidopsis. *Proc. Natl. Acad. Sci. USA* **103**, 1627-1632.

Deveaux, Y., Peaucelle, A., Roberts, G. R., Coen, E., Simon, R., Mizukami, Y., Traas, J., Murray, J. A., Doonan, J. H. and Laufs, P. (2003). The ethanol switch: a tool for tissue-specific gene induction during plant development. *Plant J.* **36**, 918-930.

Jeong, S., Trotochaud, A. E. and Clark, S. E. (1999). The Arabidopsis CLAVATA2 gene encodes a receptor-like protein required for the stability of the CLAVATA1 receptor-like kinase. *Plant Cell* **11**, 1925-1934.

Jonsson, H., Heisler, M. G., Shapiro, B. E., Meyerowitz, E. M. and Mjolsness, E. (2006). An auxin-driven polarized transport model for phyllotaxis. *Proc. Natl. Acad. Sci. USA* **103**, 1633-1638.

Kasschau, K. D., Xie, Z., Allen, E., Llave, C., Chapman, E. J., Krizan, K. A. and Carrington, J. C. (2003). P1/HC-Pro, a viral suppressor of RNA silencing, interferes with Arabidopsis development and miRNA function. *Dev. Cell* **4**, 205-217.

Laufs, P., Coen, E., Kronenberger, J., Traas, J. and Doonan, J. (2003). Separable roles of UFO during floral development revealed by conditional restoration of gene function. *Development* **130**, 785-796.

Laufs, P., Peaucelle, A., Morin, H. and Traas, J. (2004). MicroRNA regulation of the CUC genes is required for boundary size control in Arabidopsis meristems. *Development* **131**, 4311-4322.

Mallory, A. C., Reinhart, B. J., Jones-Rhoades, M. W., Tang, G., Zamore, P. D., Barton, M. K. and Bartel, D. P. (2004). MicroRNA control of PHABULOSA in leaf development: importance of pairing to the microRNA 5′ region. *EMBO J.* **23**, 3356-3364.

Moussian, B., Schoof, H., Haecker, A., Jurgens, G. and Laux, T. (1998). Role of the ZWILLE gene in the regulation of central shoot meristem cell fate during Arabidopsis embryogenesis. *EMBO J.* **17**, 1799-1809.

Nikovics, K., Blein, T., Peaucelle, A., Ishida, T., Morin, H., Aida, M. and Laufs, P. (2006). The balance between the MIR164A and CUC2 genes controls leaf margin serration in Arabidopsis. *Plant Cell* **18**, 2929-2945.

Para, A. and Sundas-Larsson, A. (2003). The pleiotropic mutation dar1 affects plant architecture in Arabidopsis thaliana. *Dev. Biol.* **254**, 215-225.

Reinhardt, D. (2005). Regulation of phyllotaxis. *Int. J. Dev. Biol.* **49**, 539-546.

Reinhardt, D., Mandel, T. and Kuhlemeier, C. (2000). Auxin regulates the initiation and radial position of plant lateral organs. *Plant Cell* **12**, 507-518.

Reinhardt, D., Pesce, E. R., Stieger, P., Mandel, T., Baltensperger, K., Bennett, M., Traas, J., Friml, J. and Kuhlemeier, C. (2003). Regulation of phyllotaxis by polar auxin transport. *Nature* **426**, 255-260.

Rhoades, M. W., Reinhart, B. J., Lim, L. P., Burge, C. B., Bartel, B. and Bartel, D. P. (2002). Prediction of plant microRNA targets. *Cell* **110**, 513-520.

Smith, H. M. and Hake, S. (2003). The interaction of two homeobox genes, BREVIPEDICELLUS and PENNYWISE, regulates internode patterning in the Arabidopsis inflorescence. *Plant Cell* **15**, 1717-1727.

Smith, R. S., Guyomarc'h, S., Mandel, T., Reinhardt, D., Kuhlemeier, C. and Prusinkiewicz, P. (2006). A plausible model of phyllotaxis. *Proc. Natl. Acad. Sci. USA* **103**, 1301-1306.

Takada, S., Hibara, K., Ishida, T. and Tasaka, M. (2001). The CUP-SHAPED COTYLEDON1 gene of Arabidopsis regulates shoot apical meristem formation. *Development* **128**, 1127-1135.

Vernoux, T., Kronenberger, J., Grandjean, O., Laufs, P. and Traas, J. (2000). PIN-FORMED 1 regulates cell fate at the periphery of the shoot apical meristem. *Development* **127**, 5157-5165.

Vroemen, C. W., Mordhorst, A. P., Albrecht, C., Kwaaitaal, M. A. and de Vries, S. C. (2003). The CUP-SHAPED COTYLEDON3 gene is required for boundary and shoot meristem formation in Arabidopsis. *Plant Cell* **15**, 1563-1577.